Journal of Molecular Catalysis A: Chemical 332 (2010) 106–112

Contents lists available at ScienceDirect

Journal of Molecular Catalysis A: Chemical

journal homepage: www.elsevier.com/locate/molcata

Ruthenium nanoparticles supported on multi-walled carbon nanotubes: Highly effective catalytic system for hydrogenation processes

Mohamad Jahjah[a], Yolande Kihn[b], Emmanuelle Teuma[a], Montserrat Gómez[a,*]

[a] Université de Toulouse, UPS, LHFA, 118 route de Narbonne, F-31062 Toulouse, France, CNRS,Bât 2R1,2ème ètage, LHFA UMR 5069, F-31062 Toulouse, France
[b] CEMES, UPR 8011 CNRS, 29 rue Jeanne Marvig 31055 Toulouse cedex 4, France

ARTICLE INFO

Article history:
Received 29 April 2010
Received in revised form 31 August 2010
Accepted 4 September 2010
Available online 15 September 2010

Keywords:
Ruthenium
Nanoparticles
Multi-walled carbon nanotubes
Hydrogenation
Recycling

ABSTRACT

Immobilization of small and homogeneously dispersed ruthenium nanoparticles stabilized by 4-(3-phenylpropyl)pyridine ligand (RuL) on functionalized multi-walled carbon nanotubes (RuL-MWCNT) have been prepared and characterized by elemental analysis and transmission electronic microscopy. A comparative hydrogenation study of unsaturated substrates using non-supported (RuL) and supported catalytic systems (RuL–MWCNT) was carried out. For all the substrates, the activity of the supported catalyst was higher towards the full hydrogenated product than that obtained using the non-supported one. Moreover, the catalytic effect of the support nature was studied using RuL immobilized on silica (RuL–SiO_2), alumina (RuL–Al_2O_3) and activated carbon (RuL–AC). The best activities and selectivities were found for RuL–MWCNT system, maintaining its catalytic behaviour upon recycling.

1. Introduction

The use of metallic nanoparticles as catalysts has undergone an exponential growth during the last decade [1–5]. In relation to the preparation of these nano-materials from salts or molecular species ("bottom up" synthetic strategy) [6], their agglomeration should be avoided using stabilizers (polymers, dendrimers, ionic liquids, ligands etc.) [7]. On the other hand, these compounds must allow the presence of active "free" surface sites in order to enhance the catalytic activity, preventing their plausible poison effect by saturation of the metallic surface [8]. This kind of nanoparticles dispersed in a liquid phase (organic, ionic liquid or aqueous solution) could exhibit an analogous behaviour to that observed using classical homogeneous catalytic systems with regard to their recycling [9,10]. Consequently, immobilization of nano-catalysts has been developed, using biphasic systems (e.g. ionic liquids) [11–13] or solid supports [14–17]. In particular, metal nanoparticles supported on a solid (commonly, carbon, inorganic oxides –such as silica, alumina, titanium dioxide – and polymeric materials) have been applied in different catalytic transformations, being easily separated from the organic product and therefore recovered to be reused [18]. It is important to note that the catalytic activity and/or selectivity could be modified depending on the support nature. More recently, multi-walled carbon nanotubes (MWCNT) have been found as appropriated catalyst support due to their significant advantages such as: (i) high catalytic activities arising from its mesoporous nature, avoiding mass transfer limitations [19]; (ii) high activity/selectivity due to the possibility to operate in the inner cavity of carbon nanotubes (confinement effect) [20]; (iii) well-defined and tuneable structure [21]; and (iv) selective growth of nanocarbons by catalytic chemical vapour deposition (C-CVD) on defined substrates to build micro-reactors [22]. In particular, metallic nanoparticles supported on MWCNT have been widely employed in the last years in hydrogenation reactions of organic compounds [23]. Palladium nanoparticles supported on MWCNT are the catalyst of choice for the hydrogenation of C=C bonds, including aromatic moieties and C≡C bonds [24]. Bimetallic Pd–Rh nanoparticles supported on carbon nanotubes catalyze effectively benzene hydrogenation at room temperature [25]. An advanced study concerning bimetallic Pt–Pd catalysts supported on MWCNT has evidenced a very good ability to hydrogenate aromatic rings in contrast to other supports [26]. With ruthenium catalysts, influence of support nature has been also proved. The reaction of three types of carbon nanofibers (CNF) has given the corresponding CNF-supported ruthenium nanoparticles and depending on the nanostructures surface of the CNF, excellent catalytic activity towards the hydrogenation of toluene has been obtained without leaching of ruthenium species, leading to a recyclable catalyst [27]. In the hydrogenation of glucose to sorbitol, ruthenium catalysts immobilized on MWCNT also showed higher catalytic activity than that obtained with the corresponding Ru catalysts immobilized on Al_2O_3 or SiO_2 [28].

* Corresponding author. Tel.: +33 561557738; fax: +33 561558204.
E-mail address: gomez@chimie.ups-tlse.fr (M. Gómez).

1381-1169/$ – see front matter © 2010 Elsevier B.V. All rights reserved.
doi:10.1016/j.molcata.2010.09.006

In a recent work, we have prepared MWCNT grafted by ionic liquids, which could be further utilized as supports of ionic liquid catalytic phase (SILCP), using a molecular rhodium precursor [29]. The resulting rhodium catalyst exhibited a significant higher activity than the corresponding SILCP supported on oxide supports and activated carbon, in the hydrogenation of 1-hexene. This catalytic behaviour could be attributed to a good dispersion of the MWCNT support in the reaction mixture that minimizes the negative effects of mass transport.

In this paper, we describe the immobilization of ruthenium nanoparticles (RuL), preformed by organometallic compound decomposition in the presence of a pyridine derivative stabilizer, and onto different supports (functionalized multi-walled carbon nanotubes, silica and activated carbon). These supported catalysts were used in the catalytic hydrogenation of several unsaturated substrates. A comparative catalytic study in terms of activity, selectivity and recycling of supported and non-supported RuL nanoparticles was purposely studied.

2. Experimental

2.1. General

Catalysts were prepared under Ar atmosphere conditions using Schlenk and Fisher–Porter bottle techniques and stocked in glovebox. THF was distilled over sodium benzophenone. Solvents were degassed under vacuum at liquid nitrogen temperature by three vacuum-argon cycles before being used. The metallic precursor [Ru(cod)(cot)] and Ru/C were purchased from NanoMeps and Aldrich, respectively. Ruthenium nanoparticles [30] and multi-walled carbon nanotubes [31] were prepared following our previously published methodologies. Al_2O_3 (Brockmann I, standard grade, neutral, 150 mesh, pore volume = 0.89 $cm^3\,g^{-1}$, Aldrich), mesoporous silica (EP10X amorphous silica, Crosfield Ltd., pore volume = 1.81 $cm^3\,g^{-1}$, particle size ≈100 μm, INEOS Silicas) and activated carbon (Sigma Aldrich) were used as supports. Other commercial chemicals were used as supplied. All hydrogenation tests were carried out in a stainless steel Top Industrie autoclave (Top 45) of 100 mL volume and capacity of 70 bar pressure, with magnetic stirring and electric heating collar. Elemental analyses were performed in a Perkin Elmer 2400 series II microanalyzer in the "Service d'Analyses du LCC" at the CNRS in Toulouse for carbon, nitrogen and hydrogen determinations. Ruthenium analysis were carried out at the "Service Central d'Analyse" in Lyon by ICP technique. Samples were dispersed in ethanol and sonicated for 5 min before dropped them onto a holey carbon copper grid and the solvent was allowed to evaporate. TEM images were obtained using a Philips CM12 microscope operating at 120 kV. GC analyses were performed on a Hewlett-Packard 5890 Series II gas chromatograph (50 m Ultra 2 capillary column) with a FID detector. Substrate conversions and products selectivity were determined by gas chromatography based on the relative area of GC-signals referred to an internal standard, calibrated to the corresponding pure compound. Enantiomeric excesses were determined by GC on FS-cyclodex-β-I/P and FS-cyclodex-α-I/P columns.

2.2. Synthesis of ruthenium nanoparticles

The preparation of RuL was based on the work previously reported [30]. A solution of 4-(3-phenylpropyl)-pyridine in THF (2 mL of a solution 0.02 M of ligand in THF, 0.04 mmol) was introduced in a Fischer–Porter bottle. The solvent was then evaporated and a solution of [Ru(cod)(cot)] (60 mg, 0.2 mmol) in THF (80 mL) was introduced under argon atmosphere. The system was next pressurized with hydrogen (1 bar) and stirred at room temperature overnight. The solvent was evaporated under vacuum. The isolated particles were further washed with pentane (3 × 10 mL). Organic phase was concentrated and analysed by ^{1}H NMR proving the absence of free ligand. The black solid was dried under reduced pressure. Yield: 93% (26.0 mg). Mean diameter = 1.31 ± 0.43 nm. IR absorptions ν_{max}/cm^{-1} 2917 and 2841 (C–H), 1612 and 1550 (C=N), 1402 and 1384 (C=C), 1258, 1089, 1019 and 798 (CO and CC of the THF).

2.3. Supported ruthenium nanoparticles

95 mg of support (MWCNT, SiO_2, Al_2O_3 or AC) were added to 5 mg (0.032 mmol) of RuL dissolved in 1 mL of THF under Ar atmosphere. The system was stirred under sonication for 2 h to form a stable black suspension. The solvent was then evaporated under vacuum. The resulting black solid was dried under reduced pressure.

2.4. Hydrogenation catalytic processes

1 mg (0.0064 mmol) of RuL or 5 mg of supported catalyst was dissolved in 1 mL of degassed ethanol. After stirring under Ar atmosphere at room temperature for 5 min, 0.64 mmol of the desired substrate was added. The resulting solution was then transferred to the autoclave, which was previously degassed three times with argon and twice with hydrogen. The catalytic mixture was pressurized with hydrogen and stirred for the reaction time. At the end of the reaction time, the reactor was degassed and the reaction mixture filtered throught Celite before GC analysis.

3. Results and discussion

3.1. Synthesis and characterization of supported ruthenium nanoparticles

The supported ruthenium nanoparticles were prepared in two steps: first, preparation of ruthenium nanoparticles stabilized by 4-(3-phenylpropyl)pyridine (RuL); second, immobilization of these particles on several solid supports (RuL-support).

The ruthenium nanoparticles RuL were synthesized by decomposition of [Ru(cod)(cot)] in the presence of the ligand and under hydrogen atmosphere, giving small (mean size: 1.31 ± 0.43 nm, Fig. 1a and b) and homogenously dispersed nanoparticles, as previously described (Scheme 1) [30]. It is important to note that full decomposition of the organometallic precursor ([Ru(cod)(cot)]) is achieved after ca. 18 h at room temperature under 3 bar of hydrogen, checked by NMR (organic solution analysis) in agreement with the high yield to give RuL (more than 90% for each ruthenium nanoparticles synthesis). In addition, kinetic measurements monitored by ^{1}H NMR under hydrogen pressure, evidenced the total hydrogenation of coordinated olefins to give cyclooctane [30].

Once the particles were isolated, they were supported on commercial supports (alumina, silica and activated carbon: RuL–Al_2O_3, RuL–SiO_2, RuL–AC) and also on functionalized multi-walled carbon nanotubes (RuL–MWCNT). The MWCNT used in this work were prepared by C-CVD [31] and further functionalized by nitric acid treatment, giving mainly carboxylic acid groups but also carbonyl, quinine and phenol groups on their surface [32]. Full characterization of these MWCNT has been described in our previous contribution [29]. The RuL immobilization on the support was carried out by addition of ruthenium nanoparticles dispersed in THF on the solid support, followed by ultrasound treatment. The solvent was then removed under reduced pressure to isolate the material as a black powder. For RuL–MWCNT, several loads of RuL in relation to the support were used (5, 10 or 40 mg of RuL per 100 mg of MWCNT). For the commercial supports, 10 mg of RuL per 100 mg

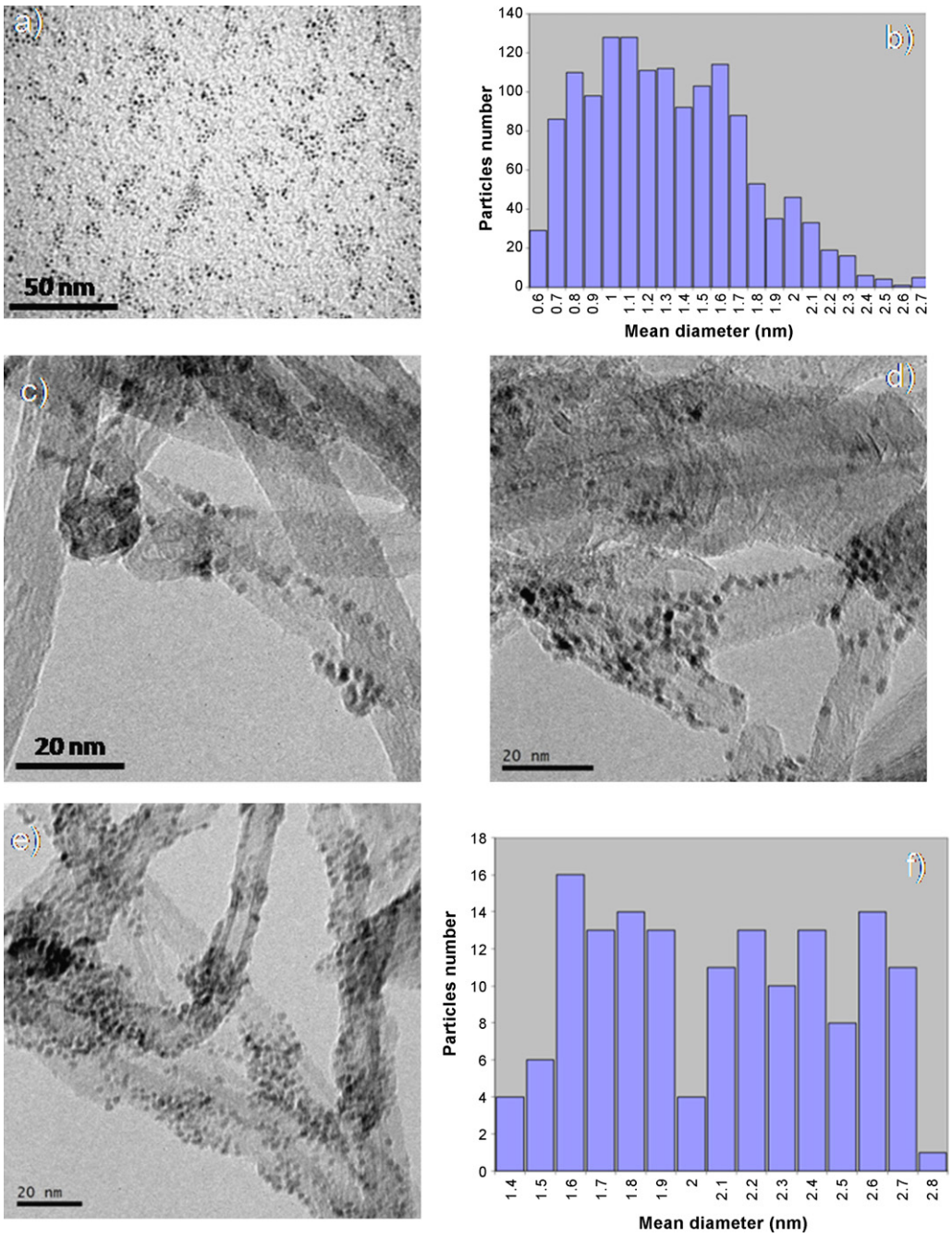

Fig. 1. TEM micrographs of RuL (a) and their size distribution (d_{mean} = 1.31 ± 0.43 nm for 1417 counted particles) (b) and supported RuL–MWCNT materials for different RuL weight loads (c–e): (c) 5% (d_{mean}(RuL) = 2.01 ± 0.39 nm for 30 counted particles); (d) 10% (d_{mean}(RuL) = 1.87 ± 0.29 nm for 30 counted particles); and (e) 40% (d_{mean}(RuL) = 2.09 ± 0.39 nm for 150 counted particles) and the corresponding size distribution (f).

of support was only used. After supporting, the stabilizing ligand L remained in the composition of the ruthenium nanoparticles, as evidenced by elemental analysis (Table 1).

Concerning RuL–MWCNT systems, the ruthenium nanoparticles did not exhibit important difference with the RuL load increase in relation to the support (mean diameter ca. 2.0 nm), showing spherical shapes and a quite homogeneous dispersion on the support without aggregates formation (Fig. 1c and e); but their mean size

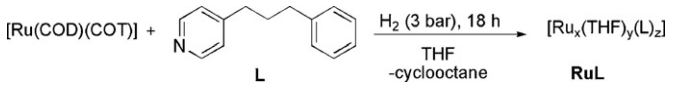

Scheme 1. Synthesis of Ru nanoparticles stabilized by L, RuL.

Table 1
Elemental analysis (weight percentage of Ru, C, H and N) of RuL-support materials.

RuL-support[a]	Ru	C	H	N
RuL–MWCNT (5%)	2.38	86.0	0.25	0.30
RuL–MWCNT (10%)	4.63	86.4	0.30	0.28
RuL–MWCNT (40%)	21.65	65.7	1.10	0.73
RuL–Al_2O_3 (10%)	6.20	2.12	0.54	0.14
RuL–SiO_2 (10%)	6.62	2.33	0.20	0.17
RuL–AC (10%)	3.11	79.1	1.20	0.56

[a] In brackets, weight percentage of RuL in relation to the support.

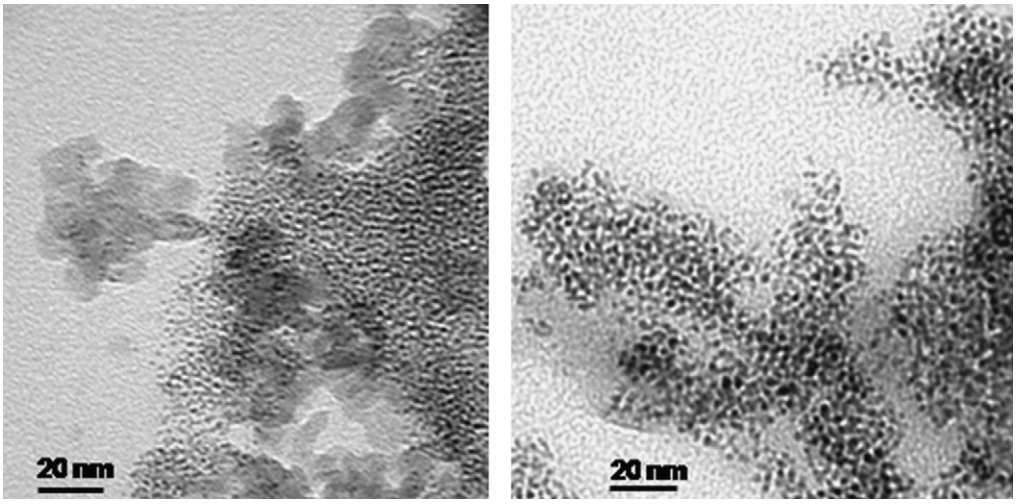

Fig. 2. TEM micrographs of RuL–SiO_2 (left) and RuL–Al_2O_3 (right).

is rather higher than that observed before immobilization (Fig. 1a and b), although the relative population remains distant. For the nanocomposite containing 40% RuL load, two particles populations could be distinguished at ca. 1.8 nm and 2.4 nm (Fig. 1e and f); for the other RuL–MWCNT systems (5% and 10% RuL loads), few numbers of particles could be counted for the determination of their mean size, giving in these two cases more uncertainty. Considering a compact packing arrangement (as presented by the bulk metal) of spherical nanoparticles, a cluster estimated composition of Ru_{85} (mean diameter ca. 1.3 nm) can be proposed for non-supported nanoparticles RuL and of Ru_{309} (mean diameter ca. 2.0 nm) for the supported ones (RuL–MWCNT). By means of "magic number" approach [33], we can guess that up to 62% (for 3-shell nanoclusters, 147 atoms) and 52% (for 4-shell nanoclusters, 309 atoms) of metal atoms are placed on the metallic surface.

Ruthenium nanoparticles supported on silica and alumina exhibited an important tendency to be agglomerated as observed by the corresponding TEM micrographs (Fig. 2); for both supports, the mean diameter of RuL is close to that observed for the nanoparticles supported on multi-walled carbon nanotubes (ca. 2 nm).

3.2. Catalytic hydrogenation

A comparative hydrogenation study using supported (RuL–MWCNT) and non-supported (RuL) catalysts was carried out for several substrates (Scheme 2), in order to prove the support influence in the catalytic reaction. The results are collected in Table 2.

For the non-activated olefin methyl oleate (substrate 2), slight differences were observed between both kind of catalysts (entries 3 and 4, Table 2). However, for the other functionalized substrates, Ru-supported nanoparticles were definitively more active (entries 2, 6, 8, 10 and 12 versus 1, 5, 7, 9 and 11, respectively, Table 2).

In particular, for acetophenone (3) and styrene (6) hydrogenation, total substrate conversion was obtained using both types of catalytic systems (entries 5 and 6 and 11 and 12, Table 2), but for the supported catalyst only the full hydrogenated product (3a and 6a) was observed (entries 6 and 12, Table 2), in contrast to the behaviour of the non-supported catalyst which gave a mixture of hydrogenated compounds. When *p*-methylanisole (5) was used as substrate, RuL was clearly less active than RuL-MWCNT, giving only 42% substrate conversion after 18 h (entries 9 and 10, Table 2). As

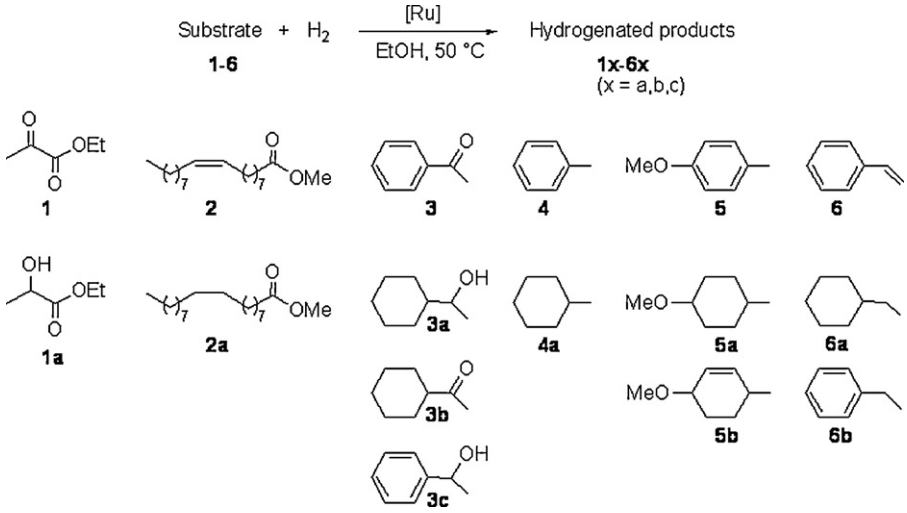

Scheme 2. Ru-catalyzed hydrogenation of unsaturated substrates (1-6) using non-supported (RuL) and supported (RuL-MWCNT) catalysts.

Table 2
Ru-catalyzed hydrogenation of 1–6 substrates, using non-supported (RuL) and MWCNT supported (RuL–MWCNT) precursors.[a]

Entry	Substrate	Catalyst	Time (h)	%Conv.[b] (Sel.)	TTO[c]	TON[d]
1	1	RuL	2.5	40	40	64.5
2	1	RuL–MWCNT	2.5	100	100	192
3	2	RuL	2	90	90	145
4	2	RuL–MWCNT	2	100	100	192
5	3	RuL	16	99 (75/15/9)[e]	74.25	120
6	3	RuL–MWCNT	16	100 (100/0/0)[e]	100	192
7	4	RuL	14	20	20	32
8	4	RuL–MWCNT	14	100	100	192
9	5	RuL	18	42 (75/25)[f]	31.5	51
10	5	RuL–MWCNT	18	100 (70/30)[f]	70	135
11	6	RuL	6	100 (75/25)[g]	75	121
12	6	RuL–MWCNT	6	100 (100/0)[g]	100	192

[a] See Scheme 2 for the products labelling. Results obtained from duplicated tests. For each substrate, the reaction time was established monitoring the consumption of hydrogen. Reaction conditions: 0.64 mmol of substrate, 0.0064 mmol of RuL, 40 bar hydrogen pressure, 50 °C.
[b] Conversions and selectivities determined by GC.
[c] Total Turnover = moles of substrate converted to full hydrogenated product per mole of catalyst (based on total metal).
[d] Turnover = moles of substrate converted to full hydrogenated product per mole of catalyst (based on ruthenium atoms on the surface, see above in the text for its determination).
[e] Chemoselectivity towards the hydrogenated products as a ratio of 3a/3b/3c.
[f] Chemoselectivity towards the hydrogenated products as a ratio of 5a/5b.
[g] Chemoselectivity towards the hydrogenated products as a ratio of 6a/6b.

expected, no reduction of the ester group was observed for the substrates 1 and 2.

Therefore, the total turnover numbers (based on the total metal amount) towards the full hydrogenated products are up to 100 for RuL–MWCNT and 75 for RuL (except for the non-activated substrate 2, entry 3, Table 2), for a constant ruthenium load. Because of only the ruthenium atoms placed on the surface are available for catalytic reactivity, these relative activities represent the lower limit and the differences between both kind of catalysts are higher taking into account the exposed ruthenium atoms; therefore, the turnover numbers (based on the ruthenium atoms on the surface) are found in the range of 135–192 for RuL–MWCNT and 32–145 for RuL. The catalytic activity enhancement of the supported (RuL–MWCNT) system in relation to the unsupported one (RuL) can be due to the substrate adsorption not only at the metal surface but also at the interface between the metal and the catalyst support as suggested by several research groups [34].

With the purpose of evaluating the chemoselectivity using RuL–MWCNT as catalyst, temperature, hydrogen pressure and substrate/metal ratio parameters were optimized for the styrene hydrogenation. RuL–MWCNT was still active under smooth conditions, at room temperature and low hydrogen pressures (even at 1 bar). Concerning the hydrogen pressure, full substrate conversion was also attained at room temperature under 25 bar hydrogen after three hours of reaction, with exclusive formation of ethylcyclohexane (6a). At lower hydrogen pressures (Fig. 3), the catalytic system remained active with total consumption of styrene using 1 bar of hydrogen, but affording a mixture of ethylbenzene and ethylcyclohexane, 6b/6a = 70/30, indicating that the catalytic system is less active under smooth conditions, favouring the faster hydrogenation that corresponds to the exocyclic C–C double bond. The pressure increase favoured the formation of the full hydrogenated product (6a), obtaining essentially ethylcyclohexane under 20 bar. These facts are in agreement with a low hydrogen solubility working at low pressures which leads to a low hydrogenation rate of styrene and in consequence the formation of ethylbenzene is favoured at 1 bar of hydrogen, in contrast to the results obtained working at higher pressure (20 bar), only obtaining the full hydrogenated product (ethylcyclohexane).

At room temperature and under 25 bar hydrogen pressure, substrate/metal ratio could be increased up to 1,000 to give full conversion of substrate with a 6b/6a ratio of 60/40 after 3 h of reaction.

In order to study the relative rate to hydrogenate the exocyclic double bond and the aromatic group, the styrene hydrogenation was examined under smooth conditions. At room temperature and under 1 bar hydrogen pressure for a substrate/ruthenium ratio of 100, the styrene hydrogenation monitoring showed the exclusive formation of ethylbenzene (6b) during the first twenty minutes of reaction; once the substrate was completely converted into ethylbenzene, the hydrogenation of the aromatic ring took place, giving exclusively ethylcyclohexane after one hour of reaction (Fig. 4). This fact is due to the different hydrogenation rate between the exocyclic double bond and the aromatic ring, being faster the hydrogenation of the olefinic function.

Effectively, these results evidence a higher catalyst activity towards the hydrogenation of the exocyclic olefin (TOF = 577 h^{-1} [35]) than that corresponding to the reduction of the aromatic ring (TOF = 288 h^{-1} [35]), different enough to permit selectively the formation of hydrogenated products, 6a and 6b.

At constant substrate/ruthenium ratio (300), an increase of ruthenium mass in relation to the support (5, 10 or 40 mg of RuL per 100 mg of MWCNT) did not improve the activity.

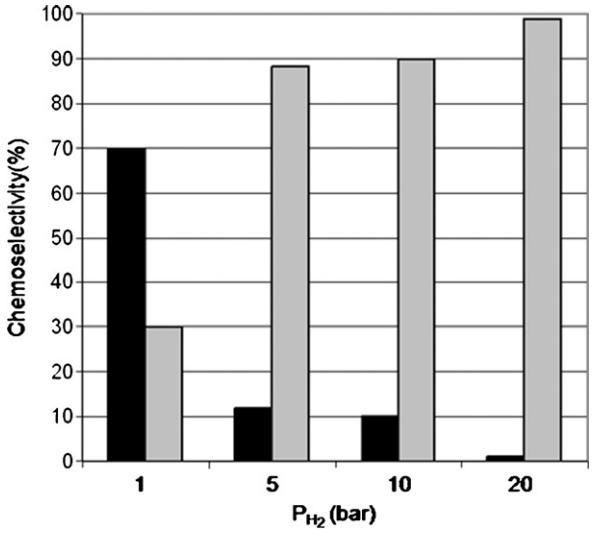

Fig. 3. Chemoselectivity for the RuL–MWCNT styrene hydrogenation, depending on the hydrogen pressure at full conversion of substrate. In black, relative percentage of ethylbenzene (6b) and in gray, ethylcyclohexane (6a).

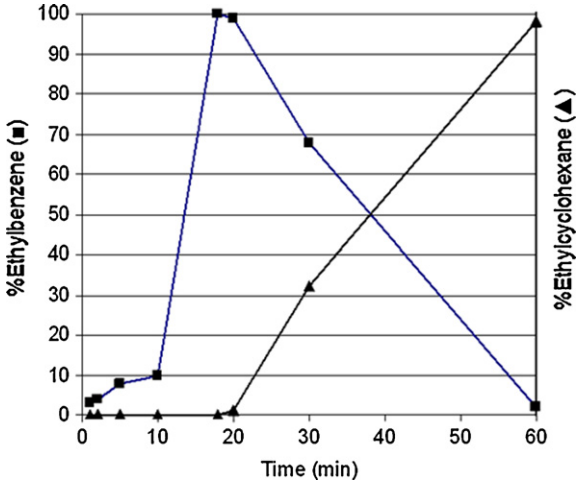

Fig. 4. RuL–MWCNT-catalyzed styrene hydrogenation monitoring.

In order to evaluate the effect of the support nature in the hydrogenation of C=C bonds, the ruthenium nanoparticles RuL were immobilized on silica, alumina and activated carbon. These materials were tested in the hydrogenation of substrates 3, 5 and 6 (Table 3). The catalytic system supported on AC gave low hydrogenation rate for the all substrates tested (entries 4, 8 and 12, Table 3). This behaviour can be associated to the high degree of microporosity of the support, leading to more important transfer mass limitations than those observed for the other supports, in spite of its large surface area. For acetophenone (3), *p*-methylanisole (5) and styrene (6), alumina was less efficient catalysts towards the full hydrogenated products (entries 3, 7 and 11, Table 3) comparing with multi-walled carbon nanotubes and silica supports (entries 1 and 2 vs. entry 3; 5 and 6 vs. entry 7; 9 and 10 vs. entry 11, Table 3). Effectively, the ethylcyclohexane/ethylbenzene ratio points to the relative activity of the different catalytic systems due to the different hydrogenation rate between both exocyclic C–C double bond and aromatic moiety. TEM analyses after styrene hydrogenation evidenced that RuNPs appear more agglomerated for alumina than for both silica and multi-walled carbon nanotubes supports (see Supplementary material), in agreement with the lower activity of RuL–Al_2O_3 catalyst compared with RuL–MWCNT and RuL–SiO_2. When commercial Ru/C was used for the hydrogenation of *p*-methylanisole, the conversion was low (entry 13, Table 3) and for the styrene hydrogenation, only ethylbenzene was formed (entry 14, Table 3), showing lower performance of the classical heterogeneous catalyst than the supported ruthenium nanoparticles, RuL.

Contrary to RuL–MWCNT, RuL–SiO_2 catalyst was not active for the styrene hydrogenation under smooth conditions (room temperature and under 1 bar hydrogen pressure for a substrate/ruthenium ratio of 100). Hydrogenation took place at room temperature but at 25 bar hydrogen pressure with a substrate/metal ratio of 200. Three consecutive additions of styrene were carried out under these conditions. A deactivation of the catalytic system was observed after the first run (entries 4–6, Table 4) by a decrease of the ethylcyclohexane/ethylbenzene selectivity, in contrast to the robustness of the catalytic system supported on multi-walled carbon nanotubes, which maintained its catalytic activity after three consecutive runs (entries 1–3, Table 4). Taking into account that the ruthenium metal content on the organic products is in all cases less than 2 ppm (determined by ICP–MS) and that the ligand used as stabilizer was not detected (checked by ^{1}H NMR), this different behaviour could be associated to an agglomeration of the nanoparticles in the case of the catalyst supported on silica.

Table 3
Ru-catalyzed hydrogenation of 3, 5 and 6 substrates, using supported precursors (RuL–MWCNT, RuL–SiO_2, RuL–Al_2O_3, RuL–AC)[a].

Entry	Substrate	Catalyst	Time (h)	%Conv.[b] (Sel.)	TTO[c]
1	3	RuL–MWCNT	16	100 (100/0/0)[d]	100
2	3	RuL–SiO_2	16	100 (100/0/0)[d]	100
3	3	RuL–Al_2O_3	16	100 (75/25/0)[d]	75
4	3	RuL–AC	16	78 (20/30/50)[d]	15.6
5	5	RuL–MWCNT	18	100 (70/30)[e]	70
6	5	RuL–SiO_2	18	100 (43/57)[e]	43
7	5	RuL–Al_2O_3	18	30 (72/28)[e]	21.6
8	5	RuL–AC	18	62 (72/28)[e]	44.6
9	6	RuL–MWCNT	6	100 (100/0)[f]	100
10	6	RuL–SiO_2	6	100 (100/0)[f]	100
11	6	RuL–Al_2O_3	6	100 (35/65)[f]	35
12	6	RuL–AC	6	100 (43/57)	43
13	5	Ru/C[g]	18	10 (80/20)[e]	12
14	6	Ru/C[g]	6	100 (0/100)[f]	100

[a] See Scheme 2 for the products labelling. Results obtained from duplicated tests. Reaction conditions: 0.64 mmol of substrate, 0.0064 mmol of RuL, 40 bar hydrogen pressure, 50 °C.
[b] Conversions and selectivities determined by GC.
[c] Total Turnover = moles of substrated converted to full hydrogenated product per mole of catalyst (based on total metal).
[d] Chemoselectivity towards the hydrogenated products as a ratio of 3a/3b/3c.
[e] Chemoselectivity towards the hydrogenated products as a ratio of 5a/5b.
[f] Chemoselectivity towards the hydrogenated products as a ratio of 6a/6b.
[g] Ru, 5% on activated carbon.

Table 4
Ru-catalyzed hydrogenation of styrene, using RuL–MWCNT and RuL–SiO_2 supported precursors.[a]

Entry	Catalyst	Styrene/Ru ratio	Run	%Conv.[b]	6a/6b ratio[b]
1	RuL–MWCNT	300	1st	100	100/0
2	RuL–MWCNT	300	2nd	100	100/0
3	RuL–MWCNT	300	3rd	100	100/0
4	RuL–SiO_2	200	1st	100	100/0
5	RuL–SiO_2	200	2nd	100	92/8
6	RuL–SiO_2	200	3rd	100	40/60

[a] See Scheme 2 for the products labelling. Results obtained from duplicated tests. Reaction conditions: 1 mmol of substrate, 25 bar hydrogen pressure, rt, 3 h.
[b] Substrate conversion and hydrogenated products ratio determined by GC.

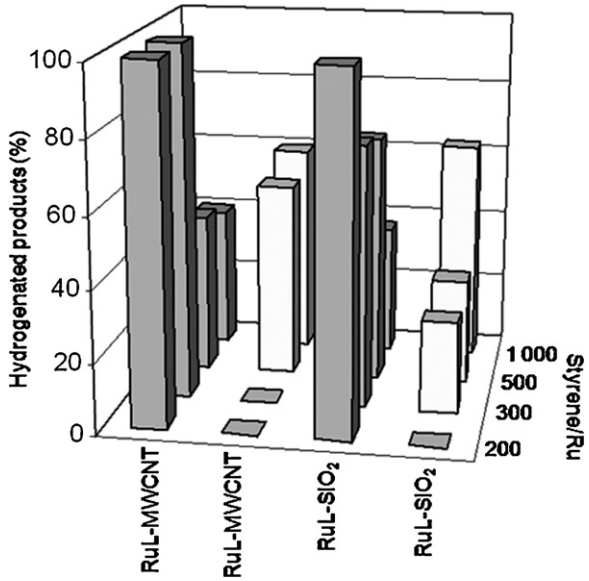

Fig. 5. Catalytic activity of RuL–MWCNT and RuL–SiO_2 for styrene hydrogenation in relation to the styrene/metal ratio at full conversion of substrate. In white, relative percentage of ethylbenzene (6b) and in gray, ethylcyclohexane (6a). (For interpretation of the references to color in the text, the reader is referred to the web version of the article.)

The catalytic activity of both systems RuL–MWCNT and RuL–SiO_2 was examined depending of the styrene/ruthenium ratio. RuL–MWCNT was more active for substrate/metal ratios in the range of 200–300 than RuL–SiO_2, showing comparable activities for more diluted systems; in particular for styrene/Ru = 1,000, both catalysts exhibited identical behaviour (Fig. 5). The catalytic systems are less active at lower metal load as evidenced by the increase of ethylbenzene in relation to the full hydrogenated product, ethylcyclohexane, favouring in consequence the product exhibiting a faster hydrogenation.

The reactivity differences observed between MWCNT and oxide supports, in particular with silica, could be due to the metallic nanoparticles arrangement on the support. While for silica, they would be preferentially located inside the pores, for multi-walled carbon nanotubes, the particles remain on the support outer surface, favouring in this case the mass transfer under catalytic conditions.

4. Conclusions

In summary, small and well-dispersed ruthenium nanoparticles supported on MWCNT were successfully used in catalytic hydrogenation reactions of unsaturated substrates. The beneficial effect of the support was proved comparing the catalytic behaviour with that corresponding to the non-supported catalyst, obtaining for all the substrates better activities using RuL–MWCNT system. Moreover, the support nature was evaluated. While Ru nanoparticles supported on alumina and activated carbon led to lower catalytic activities and chemoselectivities, silica and multi-walled carbon nanotubes supported catalysts gave preferentially the full hydrogenated products. However, only RuL–MWCNT could be reused without activity loss exclusively leading to ethylcyclohexane, in contrast to the analogous RuL–SiO_2 catalyst.

Acknowledgements

The authors thank ANR (Nanoconficat, project no. ANR-05-NANO-030), CNRS and Université Paul Sabatier for their financial support, and Prof. Philippe Serp and his team for the fruitful collaboration.

Appendix A. Supplementary data

Supplementary data associated with this article can be found, in the online version, at doi:10.1016/j.molcata.2010.09.006.

References

[1] J.D. Aiken III, R.G. Finke, J. Mol. Catal. A: Chem. A 145 (1999) 1–44.
[2] M.A. El-Sayed, Acc. Chem. Res. 34 (2001) 257–264.
[3] H. Bönnemann, R.M. Richards, Eur. J. Inorg. Chem. (2001) 2455–2480.
[4] A. Roucoux, J. Schulz, H. Patin, Chem. Rev. 102 (2002) 3757–3778.
[5] A. Roucoux, K. Philippot, Hydrogenation with Noble Metal Nanoparticles in Handbook of Homogeneous Hydrogenations, Wiley-VCH, Weinheim, 2006.
[6] G. Schmid, V.C.H. Weinheim, Clusters and Colloids, from Theory to Applications, 1994.
[7] L.S. Ott, R.G. Finke, Coord. Chem. Rev. 251 (2007) 1075–1100.
[8] Y. Li, M.A. El-Sayed, J. Phys. Chem. B 105 (2001) 8938–8943.
[9] C. Burda, X. Chen, R. Narayanan, M.A. El-Sayed, Chem. Rev. 105 (2005) 1025–1102.
[10] J. Durand, E. Teuma, M. Gómez, Eur. J. Inorg. Chem. (2008) 3577–3586.
[11] P. Migowski, J. Dupont, Chem. Eur. J. 13 (2007) 32–39.
[12] H. Olivier-Bourbigou, L. Magna, J. Mol. Cat. A: Chem. 182 (2002) 419–437.
[13] L. Duran Pachón, C.J. Elsevier, G. Rothenberg, Adv. Synth. Catal. 348 (2006) 1705–1710.
[14] M. Studer, H.-U. Blaser, C. Exner, Adv. Synth. Catal. 345 (2003) 45–65.
[15] H. Bönnemann, G.A. Braun, Chem. Eur. J. 3 (1997) 1200–1202.
[16] X. Zuo, H. Liu, D. Guo, X. Yang, Tetrahedron 55 (1999) 7787–7804.
[17] J.U. Köhler, J.S. Bradley, Langmuir 14 (1998) 2730–2735.
[18] B. Corain, P. Centomo, S. Lora, M. Kralik, J. Mol. Catal. A: Chem. 204–205 (2003) 755–762.
[19] H. Vu, F. Gonçalves, R. Philippe, E. Lamouroux, M. Corrias, Y. Kihn, D. Plee, P. Kalck, P. Serp, J. Catal. 240 (2006) 18–22.
[20] X. Pan, Z. Fan, W. Chen, Y. Ding, H. Luo, X. Bao, Nat. Mater. 6 (2007) 507–511.
[21] P. Serp, M. Corrias, P. Kalck, Catal. Appl. A. 253 (2003) 337–358.
[22] M. Ruta, I. Yuranov, P.J. Dyson, G. Laurenczy, L. Kiwi-Minsker, J. Catal. 247 (2007) 269–276.
[23] B.F.G. Johnson, Top. Catal. 24 (2003) 1–4.
[24] E.V. Starodubtseva, M.G. Vinogradov, O.V. Turova, N.A. Bumagin, E.G. Rakov, V.I. Sokolov, Catal. Commun. 10 (2009) 1441–1442.
[25] B. Yoon, H.-B. Pan, C.M. Wai, J. Phys. Chem. C 113 (2009) 1520–1525.
[26] B. Pawelec, V. La Parola, R.M. Navarro, S. Murcia-Mascarós, J.L.G. Fierro, Carbon 44 (2006) 84–98.
[27] M. Takasaki, Y. Motoyama, K. Higashi, S.-H. Yoon, I. Mochida, H. Nagashima, Chem. Asian J. 2 (2007) 1524–1533.
[28] J. Pan, J. Li, C. Wang, Z. Yang, React. Kinet. Catal. Lett. 90 (2007) 233–242.
[29] L. Rodríguez-Pérez, E. Teuma, A. Falqui, M. Gómez, P. Serp, Chem. Commun. (2008) 4201–4203.
[30] I. Favier, S. Massou, E. Teuma, K. Philippot, B. Chaudret, M. Gómez, Chem. Commun. (2008) 3296–3298.
[31] M. Corrias, B. Caussat, A. Ayral, J. Durand, Y. Kihn, P. Kalck, P. Serp, Chem. Eng. Sci. 58 (2003) 4475–4482.
[32] A. Solhy, B.F. Machado, J. Beausoleil, Y. Kihn, F. Gonçalves, M.F.R. Pereira, J.J.M. Órfão, J.L. Figueiredo, J.L. Faria, P. Serp, Carbon 46 (2008) 1194–1207.
[33] B.K. Teo, H. Zhang in, D.L. Feldheim, C.A. Foss Jr. (Eds.), Metal Nanoparticles: Synthesis, Characterization and Applications, Marcel Dekker, New York, 2002 (Chapter 3).
[34] (a) G. St-Pierre, A. Chagnes, N.-A. Bouchard, P.D. Harvey, L. Brossard, H. Ménard, Langmuir 20 (2004) 6365–6373;
(b) F. Laplante, L. Brossard, H. Ménard, Can. J. Chem 81 (2003) 258–264;
(c) G. Nery, A.M. Visco, A. Donato, C. Milone, M. Malentacchi, G. Gubitosa, Appl. Catal. A: Gen. 110 (1994) 49–59.
[35] Turnover frequency = mol of converted substrate per mol of catalyst per hour (based on Ru atoms on the surface).